Interface propagation and energy dissipation in Shape Memory Alloys

Y.J. He

Version of Record: https://www.sciencedirect.com/science/article/pii/S1359646223001446
Manuscript_02ba62b34ec0d7ec27766a0674ffe7ab

Interface propagation and energy dissipation in Shape Memory Alloys

Y. J. He

UME, ENSTA Paris, Institut Polytechnique de Paris, 91120 Palaiseau, France

Email address: yongjun.he@ensta-paris.fr

Abstract

Recent experiments showed that the macroscopic interface propagation of the martensitic phase transformation in Shape Memory Alloys (SMAs) includes unstable microstructure evolution in the macroscopic diffuse interfacial zone (with nucleation, branching, merging and/or annihilation of numerous small domains), releasing the stored energy of the diffuse interface. In this paper, with a one-dimensional Cahn-Hilliard model, a quantitative relation between the energy dissipation and the interfacial properties (interface energy and interface thickness) is revealed: the energy dissipation is governed by the energy barrier caused by the diffuse interface. The relation is verifiable with existing experiments. It can also help understand the interfacial effect on the material's fatigue failure and provide a hint to search for low-hysteresis SMAs: weak first-order phase transformation implies weak energy dissipation (low hysteresis).

Keywords: Hysteresis, interface, nonlocal effect, first-order phase transformation.

The superelasticity and shape memory effect of Shape Memory Alloys (SMAs) come from the martensitic phase transformation which belongs to the first-order phase transformation with two basic features: interface and hysteresis [1]. The hysteresis is the macroscopic reflection of the energy dissipation at the interface where the material takes the transformation between austenite and martensite. Although there are reports about the relation between hysteresis and interface [2], a clear quantitative relation verifiable with

experiments has not yet been achieved. An interface-hysteresis relation would be useful because many experiments have shown the interfacial effect on the material fatigue [3-6].

An example of the interface propagation is shown in Fig. 1 where the heating at the specimen's end of Ni-Mn-Ga single crystal drives the transformation from a martensite single variant to austenite via the macroscopic interface propagation. The diffuse interface consists of twin laminates (see the magnified view). As discussed in [7-11], such laminates can store energy that would be dissipated via the unstable microstructure evolution: the intermittent nucleation and annihilation of numerous laminates during the macroscopic interface propagation. Details about the unstable evolution can be found in the movies of [10, 11].

Another example is shown in Fig. 2 where the stress-induced martensitic phase transformation occurs via the propagation of the macroscopic domain front of the so-called "Lüders band" in the thin plate of the superelastic NiTi polycrystalline SMA [5, 6, 12, 13]. The magnified views of Fig. 2 show that the diffuse interface propagation includes nucleation, branching and merging of small bands. Such interface not only causes the energy dissipation, but also leads to the stress concentration triggering the fatigue failure. The details about the crack nucleation and fracture failure at the interfacial zone can be found in [5, 6]. Therefore, the interface energy and the macroscopic hysteresis are constantly the key issues in studying SMAs.

It is easy to estimate the hysteresis of the isothermal superelastic cycle via the stress-strain curve shown in Fig. 2, either by the stress-strain hysteresis loop area $D_{\text{hysteresis-loop}}$ or by the product of the stress hysteresis $\sigma_{hysteresis}$ and the transformation strain ε_{tr}.

$$D_{\text{cycle-dissipation}} = D_{\text{hysteresis-loop}} \approx \sigma_{hysteresis} \cdot \varepsilon_{tr} \quad (1)$$

where $\sigma_{hysteresis}$ is the difference between the two stress plateau, and the transformation strain ε_{tr} is the strain difference between austenite and martensite ($\varepsilon_{tr} = \varepsilon_{\text{Martensite}} - \varepsilon_{\text{Austenite}}$). If the energy dissipation of the forward transformation is assumed to be the same as that of the

reverse transformation, the energy dissipation density (dissipative energy per unit volume) of the material points swept by a propagating interface during the forward (or reverse) transformation should be

$$\mathrm{D}_{\mathrm{interface-propagation}} \approx \frac{\mathrm{D}_{\mathrm{hysteresis-loop}}}{2} \approx \frac{\sigma_{hysteresis} \cdot \varepsilon_{tr}}{2} \tag{2}$$

Then the key question to answer in this paper is: can the interface energy be related to this dissipation $\mathrm{D}_{\text{interfce-propagation}}$? Before quantifying the interface energy and relating it to $\mathrm{D}_{\text{interfce-propagation}}$, we first discuss why an interface is needed during the phase transformation.

There is a consensus in literature [14-20]: the interface formation is an attribute for the materials with non-convex strain energy or "up-down-up" softening stress-strain curve (σ-ε curve) as shown in Fig. 3(a) and 3(b). It is generally assumed in the insert (i) of Fig. 3(a) that each stress plateau is associated with a softening σ-ε curve [20-22]. More importantly, the relation between the stress plateau and the softening curve has been identified in the experiments on NiTi polycrystalline SMA in [19] as shown in Fig. (3a): they measured the stress plateau ($\sigma_{\text{upper-plateau}} \approx 370$ MPa) of the *non-uniform* deformation of the specimen (with interface propagation), and the softening stress-strain curve of the specimen's *uniform* deformation (without interface propagation). The measurement of the softening curve needs special designs to achieve the specimen's uniform deformation; more technical details can be found in [19]. Based on the softening σ-ε curve in Fig. 3(a), the non-convex strain energy density f can be obtained by the integration Eq. (3) and plotted in Fig. 3(b).

$$f(\varepsilon) = \int_0^{\varepsilon} \sigma(\varepsilon)\, d\varepsilon \tag{3}$$

The relation between the non-convex energy and the SMA's superelasticity has been well discussed [16]. Particularly, there is a special line (so-called Maxwell line) touching the two convex parts of the energy curve (see Fig. 3(b)). The slope of the Maxwell line is called Maxwell stress, under which austenite and martensite can co-exist because the two phases have equal Gibbs free energy under the Maxwell stress ($g=f - \sigma_{\text{Maxwell}} \cdot \varepsilon$) as shown in Fig. 3(c)

where the amplitude of the energy barrier separating the two equilibrium phases is $\Delta g_0 \approx 1.1$ MPa (or 10^6 J/m^{-3}).

One might guess that this energy barrier should be related to the energy dissipation of the phase transformation. However, the softening stress-strain curve associated with the non-convex energy curve was measured for the *uniform* deformation of the specimen [19]. That means, all the material points of the specimen deform macroscopically *simultaneously*. By contrast, in the normal experiments of the stress-induced martensitic phase transformation, the specimen takes *non-uniform* deformation with the interface propagation: the material points take the phase transformation *sequentially* during the interface propagation along the specimen. In other words, when a material point is taking the phase transformation, its neighboring points would give certain constraints on it due to their deformation difference or misfit. Such deformation misfit leads to the formation of the complex microstructures in the diffuse interfacial zones in Fig. 1 and Fig. 2. That means, besides the energy barrier due to the softening property (Δg_0 in Fig. 3(c)), there is extra energy for the deformation misfit in the interfacial zone.

The deformation misfit energy can be estimated by microstructure formation (branching/hierarchical laminates/bands) [2, 7-9, 23] or by macroscopic elasticity [24]. By contrast, in order to obtain a simple and clear interface-hysteresis relation here, I adopt the macroscopic continuum theory taking the lump-sum global effect of the deformation misfit as a kind of non-local effect: the energy of a material point depends not only on its own deformation state (strain ε), but also on the deformation states of its neighbors. A simple version of the non-local theory is the gradient theory (or Ginzburg-Landau theory) which was adopted to study the interfacial properties of the phase transformable materials [25-30]. In this paper, I mainly follow the spirit of [25, 26] to drive the interface energy with the one-dimensional model shown in Fig. 4.

The macroscopic strain gradually changes in the interfacial zone (Fig. 4(a)), and the energy density $u(\varepsilon, \varepsilon')$ includes two parts: the local energy $u_{\text{local}}(\varepsilon)$ is from the Gibbs free energy shown in Fig. 3(c) and plotted in Fig 4(b) with $u_{\text{local}}(\varepsilon)=\Delta g(\varepsilon)=g(\varepsilon)-g_{\text{Martensite}}$; the nonlocal energy is the strain gradient energy $u_{nonlocal}(\varepsilon') = k(\varepsilon')^2 = k\left(\frac{d\varepsilon}{dx}\right)^2$, where k is the gradient coefficient and x is the coordinate of the specimen's length direction. According to [25], the interface energy can be expressed as

$$U_{interface} = \int_{-\infty}^{+\infty} u(\varepsilon, \varepsilon')\, dx$$

$$= \int_{-\infty}^{+\infty} [u_{local}(\varepsilon) + u_{non-local}(\varepsilon')]\, dx = \int_{-\infty}^{+\infty} \left[\Delta g(\varepsilon) + k\left(\frac{d\varepsilon}{dx}\right)^2\right] dx \quad (4)$$

Euler-Lagrange equation [25, 31] is adopted to minimize the interface energy for the equilibrium state:

$$u_{local} = \Delta g(\varepsilon) = k(\varepsilon')^2 = u_{non-local} \quad (5)$$

Detailed derivation of Eq. (5) is in Appendix. Equation (5) means that the local energy u_{local} of each material point at the equilibrium interfacial zone is equal to its non-local energy $u_{non\text{-}local}$. This conclusion was also obtained in [25, 26]. Therefore, the energy density $u(\varepsilon, \varepsilon')$ is two times of the local energy.

$$u(\varepsilon) = 2u_{local} = 2\Delta g(\varepsilon) \quad (6)$$

So, the energy distribution in the equilibrium interfacial zone can be obtained as $u(\varepsilon)$ in Figs 4(c) and $u(x)$ in Fig. 4(d) where the amplitude of the energy barrier separating the two phases is $u_{\text{barrier}} = 2\Delta g_0 \approx 2.2$ MPa. Similar to [25], the thickness of the interfacial zone $l_{\text{interface}}$ in Fig. 4(a) can be estimated via the maximum slope of the strain profile $\left(\frac{d\varepsilon}{dx}\right)_{max}$.

$$l_{interface} = \frac{\varepsilon_{tr}}{\left(\frac{d\varepsilon}{dx}\right)_{max}} = \varepsilon_{tr}\sqrt{\frac{k}{\Delta g_0}} \quad (7)$$

The relation $\left(\frac{d\varepsilon}{dx}\right)_{max} = \sqrt{\frac{\Delta g_0}{k}}$ according to Eq. (5) has been adopted in the Eq. (7). The gradient coefficient k is hardly measured experimentally, while the interface thickness can be measured easily. So, rearranging Eq. (7) leads to the expression of the gradient coefficient k with the interface thickness:

$$k = \Delta g_0 \left(\frac{l_{interface}}{\varepsilon_{tr}}\right)^2 \tag{8}$$

Substituting Eqs. (5) and (8) into Eq.(4), the interface energy can be expressed:

$$U_{interface} = 2\int_{\varepsilon_A}^{\varepsilon_M}\left[\sqrt{\Delta g(\varepsilon)k}\right]d\varepsilon \tag{9}_1$$

$$= C \cdot 2\Delta g_0 \cdot l_{interface} \tag{9}_2$$

where $C = \frac{1}{\varepsilon_{tr}}\int_{\varepsilon_A}^{\varepsilon_M}\sqrt{\frac{\Delta g(\varepsilon)}{\Delta g_0}}d\varepsilon$

Detailed derivation of Eq. (9) can be found in Appendix. The parameter C is in the range $0 \leq C \leq 1$ because $0 \leq \frac{\Delta g(\varepsilon)}{\Delta g_0} \leq 1$ when $\varepsilon_{Austenite} \leq \varepsilon \leq \varepsilon_{Martensite}$ as shown in Fig. 4(b). The detailed dependence of C on $\Delta g(\varepsilon)$ is discussed in the Appendix. Equation $(9)_2$ indicates that the interface energy is proportional to the interface thickness, which agrees with [24, 25]. That means, the larger interfacial zone stores larger energy. With Eq. $(9)_2$, the energy barrier, u_{barrier}, can be estimated by the interface energy and the interface thickness:

$$u_{barrier} = 2\Delta g_0 = \frac{1}{C}\cdot\frac{U_{interface}}{l_{interface}} \tag{10}$$

It is natural to conjecture that the energy dissipation of the phase transformation is equal to the energy barrier. That is to say, the combination of Eqs. (2) and (10) leads to the relation between the energy dissipation (hysteresis) and the interfacial properties:

$$\frac{\mathrm{D}_{\mathrm{hysteresis-loop}}}{2} = \frac{\sigma_{hysteresis}\cdot\varepsilon_{tr}}{2} = \mathrm{D}_{\mathrm{interface-propagation}} \approx u_{barrier} = 2\Delta g_0 = \frac{1}{C}\cdot\frac{U_{interface}}{l_{interface}} \tag{11}$$

Equation (11) can be justified by the existing experiments of NiTi polycrystalline SMAs whose isothermal hysteresis loop (or the product of the stress hysteresis and the

transformation strain) give the values of $D_{interface-propagation}$ within the range (3 MPa ~ 5 MPa) [12, 32, 33]. Equation (11) provides two methods for estimating the barrier $u_{barrier}$: one is via the softening property (Δg_0); the other is via the ratio of the interface energy to the interface thickness ($\frac{U_{interface}}{l_{interface}}$).

An example of the first method can be seen by Fig. 3(c) where $\Delta g_0 \approx 1.1$ MPa; then $u_{barrier} = 2\Delta g_0 \approx 2.2$ MPa, which is little bit lower than $D_{interface-propagation}$ (3 MPa ~ 5 MPa). That is understandable if we note that the derivation of the interfacial properties in Eq. (11) is based on the equilibrium state by minimizing the interface energy in Eqs. (4) and (5). In the real experiment of Fig. 3(a), the interface propagation of the phase transformation occurs at the stress plateau ($\sigma_{\text{upper-plateau}} \approx 370$ MPa) rather than the Maxwell stress ($\sigma_{\text{Maxwell}} \approx 354$ MPa). Figure 3(d) indicates that austenite and martensite have different Gibbs free energy under the plateau stress ($g^* = f - \sigma_{upper-plateau} \cdot \varepsilon$). That means, the phase transformation is a nonequilibrium process. In Fig. 3(d), the local energy barrier $\Delta g_0^* \approx 1.8$ MPa, meaning that the energy released from the barrier peak (with the maximum local stored energy density) to martensite. If the condition of Eq (5) is still approximately satisfied ($u_{local} = u_{non-local}$), the interfacial energy barrier $u_{barrier} = 2\Delta g_0^* \approx 3.6$ MPa, which basically agrees with $D_{interface-propagation}$ (3 MPa ~ 5 MPa). It is seen that the nonequilibrium concept should help give more accurate relation. However, the consideration of the nonequilibrium dynamic interface propagation and the associated microstructure evolution needs more advanced mathematics [34, 35]. By contrast, in current study based on equilibrium concepts, a simple and clear relation between the energy dissipation and the interfacial properties can be obtained in Eq. (11).

The second method for estimating the interfacial energy barrier of Eq. (11) can be demonstrated via the elastic misfit energy at the domain front of NiTi polycrystalline SMA [24] where the ratio of the deformation misfit energy to the interface thickness is around

1MPa. In this paper, the deformation misfit energy is taken as the nonlocal energy, and the nonlocal energy needs to be equal to the local non-convex energy in Eq.(5). So, the ratio $\frac{U_{interface}}{l_{interface}}$ should be around 2 MPa. Then, according to Eq. (11), $\mathrm{D}_{\mathrm{interface-propagation}} \approx u_{barrier} = \frac{1}{C} \cdot \frac{U_{interface}}{l_{interface}} = 3\mathrm{MPa}$, taking the parameter C=2/3 (the reason for C=2/3 can be found in Appendix). In summary, both methods (via the softening Δg_0 and via the ratio $\frac{U_{interface}}{l_{interface}}$) can approximately estimate the energy dissipation of the propagating interface.

The implication of Eq. (11) can be demonstrated by the energy profile $u(x)$ in Fig. 4(d) where the barrier peak represents the maximum stored energy density in the interfacial zone. During the interface propagation, a material point needs to store energy gradually up to $2\Delta g_0$ and then release (dissipate) the energy. It is also implied that the higher stored energy at the interface leads to higher stress concentration, triggering the defect formation and fatigue failure at the interface [5, 6]. Therefore, there are several reports about the improvement of SMAs' fatigue behaviors by reducing the interface energy. For example, the interfacial deformation misfit energy can be reduced to almost zero according to the geometric compatibility criterion (so-called "middle eigenvalue λ_2 equal to 1" or "cofactor condition") [2, 3, 36]. Although this geometric compatibility criterion has obtained great success in guiding the search for new low-hysteresis SMAs, there are still some doubts and "abnormal" cases. For example, in the comparative study on the alloys $Zn_{45}Au_xCu_{55-x}$ [4], the alloy with x=27 has small hysteresis, but its λ_2 is not close to 1. On the other hand, if there was a SMA perfectly satisfying the geometric compatibility (i.e., $k \rightarrow 0$ in current model), its interface energy should approach zero according to Eq. $(9)_1$. But, it would also have a small interface thickness $l_{\mathrm{interface}}$ as predicted in Eq. (7). So, its interfacial energy barrier related to the ratio $\frac{U_{interface}}{l_{interface}}$ in Eq. (11) might not approach zero. More importantly, the energy barrier of the non-convex energy (Δg_0), which is independent of the geometric compatibility, always causes

energy dissipation when a material point takes the phase transformation across the interfacial zone (no matter how narrow the interfacial zone is). Therefore, the sufficient and necessary condition for low hysteresis should not be the geometric compatibility alone.

In fact, the relation between Δg_0 and the energy dissipation in Eq. (11) implies a possible new low-hysteresis criterion: low hysteresis can be achieved by weak softening (small Δg_0). The inserts (ii) and (iii) of Fig. 3(a) graphically show the relation between the softening stress-strain curve and the energy barrier: the area A2 (or A4) enclosed by the softening curve and the Maxwell line (or the stress plateau) represent the non-convex energy barrier Δg_0 in Fig. 3(c) (or Δg_0^* in Fig. 3(d)). So, the weak softening means that the softening curve is very close to the Maxwell line or the stress plateau. In literature, the softening has been also studied by microscopic experiments [37, 38] and atomic modeling such as first-principle methods [1, 39]. Particularly, the first-principle calculation on the very small energy barrier of *weak* first-order phase transformation [1] was adopted to explain the extremely small hysteresis of AuZn in the experiment [37]. Interestingly, if the energy barrier disappeared completely, the phase transformation might change from first-order transition to second-order transition where there is neither interface nor hysteresis.

In summary, the macroscopic interface propagation includes unstable dissipative microstructure evolution releasing the stored energy in the diffuse interfacial zone (Figs. (1) and (2)). The origin of the interface formation is the non-convex energy or the softening stress-strain curve (Fig. (3)) which implies the energy barrier in the diffuse interface (Fig. 4). With the one-dimensional Cahn-Hilliard model, the simple interface-hysteresis relation is obtained (Eq. (11)) which can help understand the interfacial effect on the fatigue failure and provide a hint to search for low-hysteresis SMAs.

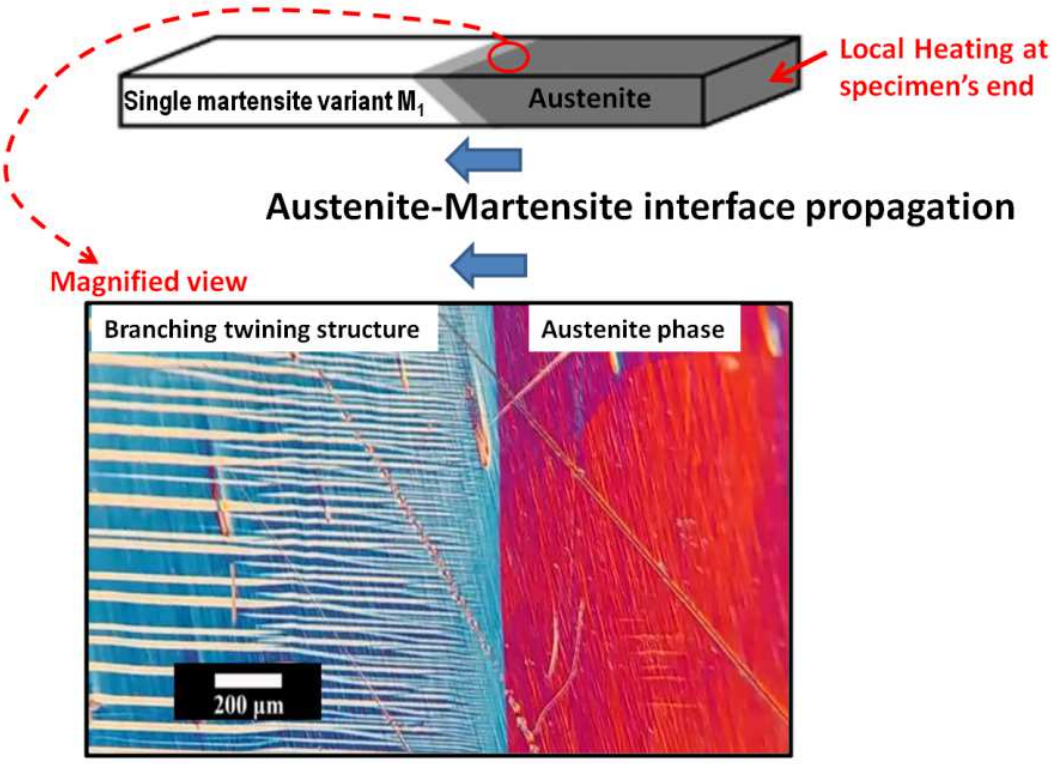

Figure 1. The interfacial zone of the heating-induced transformation from a martensite variant (denoted as M_1) to austenite in Ni-Mn-Ga single crystal SMA.

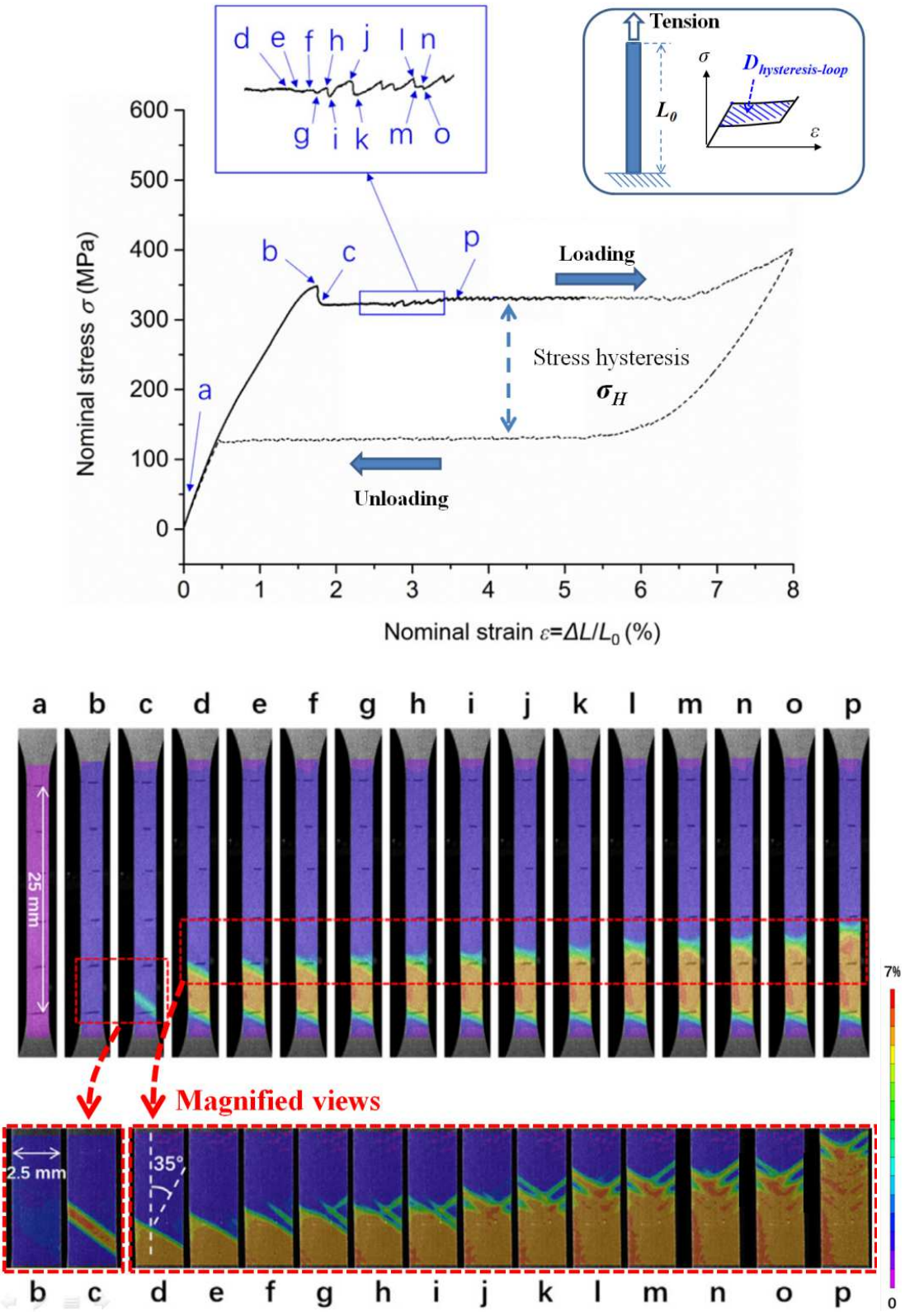

Figure 2. The branching domain front of the Lüders band of the stress-induced austenite → martensite phase transformation is demonstrated by the DIC strain maps (Digital Image Correlation) of the thin plate/strip of the superelatic NiTi polycrystalline SMA.

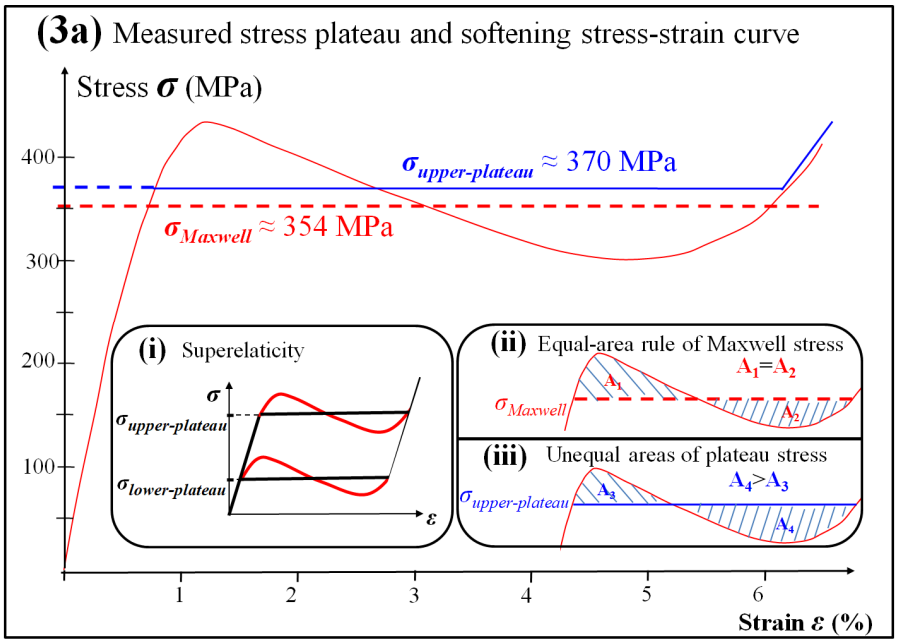
(3a) Measured stress plateau and softening stress-strain curve
Stress σ (MPa)
σupper-plateau ≈ 370 MPa
σMaxwell ≈ 354 MPa
(i) Superelaticity
σupper-plateau
σlower-plateau
ε
(ii) Equal-area rule of Maxwell stress
A1=A2
σMaxwell
(iii) Unequal areas of plateau stress
A4>A3
σupper-plateau
Strain ε (%)

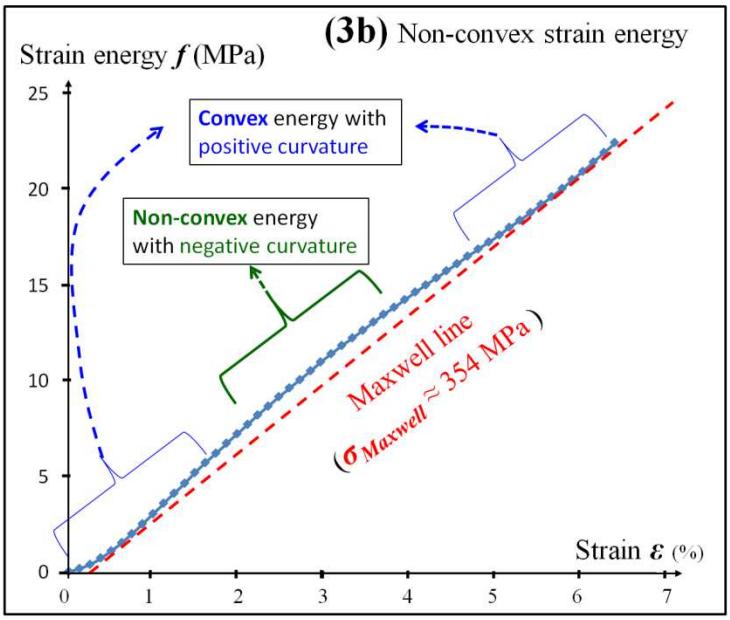
(3b) Non-convex strain energy
Strain energy f (MPa)
Convex energy with positive curvature
Non-convex energy with negative curvature
Maxwell line
(σMaxwell ≈ 354 MPa)
Strain ε (%)

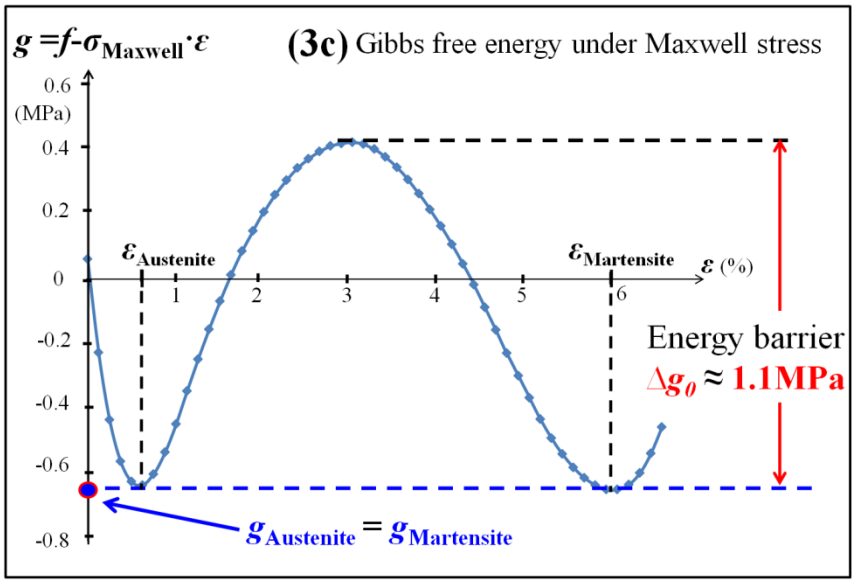
g = f - σMaxwell·ε
(3c) Gibbs free energy under Maxwell stress
(MPa)
εAustenite
εMartensite
ε (%)
Energy barrier
Δg0 ≈ 1.1MPa
gAustenite = gMartensite

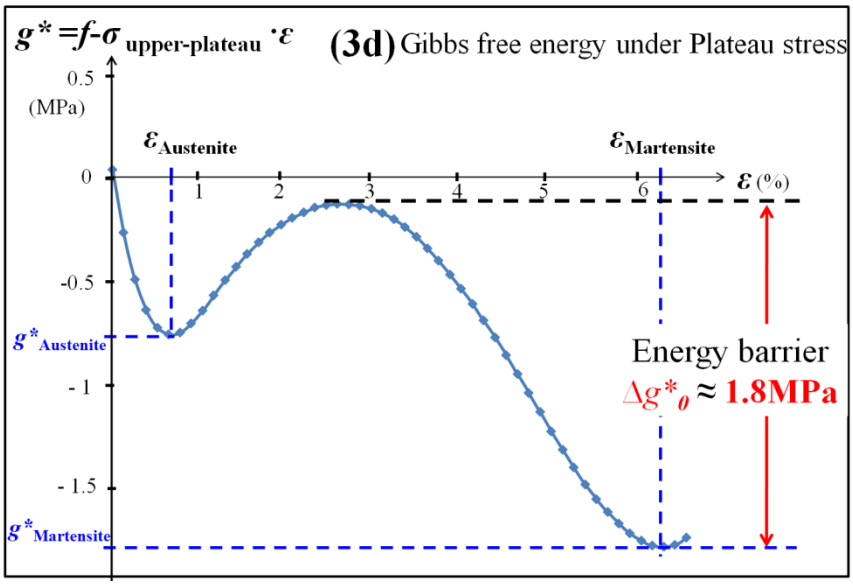

Figure 3. (a) Experimental plateau stress and softening stress-strain curve (data from [19]); (b) Non-convex strain energy derived from the softening stress-strain curve via Eq. (3); (c) Gibbs free energy under Maxwell stress; (d) Gibbs free energy under plateau stress.

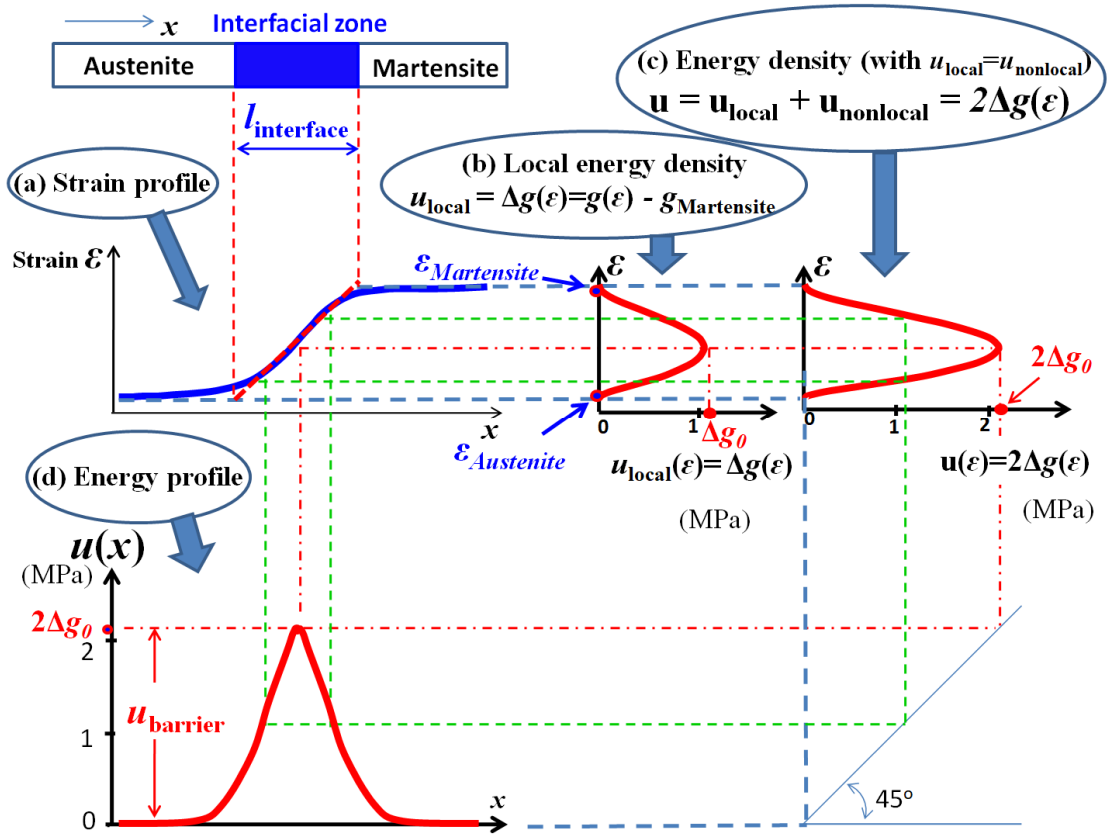

Figure 4. Schematic equilibrium interfacial properties: (a) strain profile; (b) local energy u_{local}; (c) energy density u including local and nonlocal energy (with the relation $u_{local} = u_{non-local}$ in Eq. (5)); (d) Energy profile with the energy barrier u_{barrier}.

References:

[1] M. Sanati, R. C. Albers, T. Lookman, A. Saxena, First-order versus second-order phase transformation in AuZn, Phys. Rev. B 88 (2013) 024110.

[2] Z. Zhang, R. D. James, S. Muller, Energy barriers and hysteresis in martensitic phase transformations, Acta Materialia 57 (2009) 4332-4352.

[3] H. Shi, R. Delville, V. Srivastava, R.D. James, D. Schryvers, Microstructural dependence on middle eigenvalue in Ti–Ni–Au, Journal of Alloys and Compounds 582 (2014) 703–707.

[4] Y. Song, X. Chen, V. Dabade, T. W. Shield, R. D. James, Enhanced reversibility and unusual microstructure of a phase-transforming material, Nature, 502 (2013) 85–88.

[5] S. Zhang, Y.J. He, Fatigue resistance of branching phase-transformation fronts in pseudoelastic NiTi polycrystalline strips, International Journal of Solids and Structures 135 (2018) 233-244.

[6] L. Zheng, Y.J. He, Z. Moumni, Lüders-like band front motion and fatigue life of pseudoelastic polycrystalline NiTi shape memory alloy, Scripta Materialia 123 (2016) 46–50.

[7] R.V. Kohn, S. Müller, Branching of twins near an austenite—twinned-martensite interface, Philos. Mag. A 66 (5) (1992) 697–715.

[8] E. Bronstein, E. Faran, D. Shilo, Analysis of austenite-martensite phase boundary and twinned microstructure in shape memory alloys: The role of twinning disconnections, Acta Materialia 164 (2019) 520-529.

[9] H. Seiner, P. Plucinsky, V. Dabade, B. Benešová , R. D. James, Branching of twins in shape memory alloys revisited, Journal of the Mechanics and Physics of Solids 141 (2020) 103961.

[10] C. Zhang, G. Qin, S. Zhang, X. Chen, Y. J. He, Hysteresis effect on austenite-martensite interface in Ni-Mn-Ga single crystal, Scripta Materialia 222 (2023) 115029.

[11] G. Qin, C. Zhang, S. Zhang, X. Chen, Y. J. He, Compatibility effect on stress-free two-way memory of Ni-Mn-Ga single crystal, Journal of Alloys and Compounds 935 (2023) 168134.

[12] J. A. Shaw, S. Kyriakides, On the nucleation and propagation of phase transformation fronts in a NiTi alloy, Acta mater. 45 (1997) 683-700.

[13] X. Zhang, P. Feng, Y.J. He, T. Yu, Q.P. Sun, Experimental study on rate dependence of macroscopic domain and stress hysteresis in NiTi shape memory alloy strips, International Journal of Mechanical Sciences 52 (2010) 1660-1670.

[14] J. L. Ericksen, Equilibrium of bars, Journal of Elasticity 5 (1975) 191–201.
[15] R. D. James, The propagation of phase boundaries in elastic bars. Archive for Rational Mechanics and Analysis 73 (1980) 125-158.
[16] F. Falk, Model free energy, mechanics, and thermodynamics of shape memory alloys, Acta Metallurgica 28 (1980) 1773–1780.
[17] R. Abeyaratne and J. K. Knowles, Kinetic Relations and the Propagation of Phase Boundaries in Solids, Arch. Rational Mech Anal. 114 (1991) 119-154.
[18] Y. J. He, Q. P. Sun, Effects of structural and material length scales on stress induced martensite macrodomain patterns in tube configurations, International Journal of Solids and Structures 46 (2009) 3045-3060.
[19] J.F. Hallai, S. Kyriakides, Underlying material response for Lüders-like instabilities, International Journal of Plasticity 47 (2013) 1-12.
[20] A. Duval, M. Haboussi, T. Ben Zineb, Modelling of localization and propagation of phase transformation in superelastic SMA by a gradient nonlocal approach, International Journal of Solids and Structures 48 (2011) 1879–1893.
[21] D. Jiang, S. Kyriakides, C. M. Landis, K. Kazinakis, Modeling of propagation of phase transformation fronts in NiTi under uniaxial tension, European Journal of Mechanics A/Solids 64 (2017) 131-142.
[22] S. Stupkiewicz, M. Rezaee-Hajidehi, H. Petryk, Multiscale analysis of the effect of interfacial energy on non-monotonic stress–strain response in shape memory alloys, International Journal of Solids and Structures 221 (2021) 77–91.
[23] S. Stupkiewicz, G. Maciejewski, H. Petryk, Low-energy morphology of the interface layer between austenite and twinned martensite, Acta Materialia 55 (2007) 6292–6306.
[24] L. Dong, R. H. Zhou, X.L. Wang, G. K. Hu, Q. P. Sun, On interfacial energy of macroscopic domains in polycrystalline NiTi shape memory alloys, International Journal of Solids and Structures 80 (2016) 445–455.
[25] J. W. Cahn, J. E. Hilliard, Free energy of a nonuniform system I. Interfacial free energy, The Journal of Chemical Physics 28 (1958) 258–267.
[26] F. Falk, Ginzbur–Landau theory of static domain-walls in shape-memory alloys, Z. Physik B – Condensed Matter 51 (1983) 177–185.
[27] K. O. Rasmussen, T. Lookman, A. Saxena, A. R. Bishop, R. C. Albers, S. R. Shenoy, Three-dimensional elastic compatibility and varieties of twins in martensites, Physical Review Letters 87 (2001) 055704.

[28] V. I. Levitas, D.-W. Lee, D. L. Preston, Interface propagation and microstructure evolution in phase field models of stress-induced martensitic phase transformations, International Journal of Plasticity 26 (2010) 395–422.

[29] Q. Peng, Y.J. He, Z. Moumni, A phase-field model on the hysteretic magneto-mechanical behaviours of ferromagnetic shape memory alloy, Acta Materialia 88 (2015) 13–24.

[30] M. Rezaee-Hajidehia , K. Tůmab, S. Stupkiewicz, Gradient-enhanced thermomechanical 3D model for simulation of transformation patterns in pseudoelastic shape memory alloys, International Journal of Plasticity 128 (2020) 102589.

[31] H. Margenau, G. M. Murphy, The mathematics of physics and chemistry, Second edition, D. Van Nostrand Company, Inc. Princeton, New Jersey 1956.

[32] Y.J. He, H. Yin, R. Zhou, Q. P. Sun, Ambient effect on damping peak of NiTi shape memory alloy, Materials Letters 64 (2010) 1483-1486.

[33] H. Yin, Y.J. He, Q. P. Sun, Effect of deformation frequency on temperature and stress oscillations in cyclic phase transition of NiTi shape memory alloy, Journal of the Mechanics and Physics of Solids 67 (2014) 100–128.

[34] J. M. Ball, P. J. Holmes, R. D. James, R. L. Pego, P. J. Swart, On the Dynamics of Fine Structure. J. Nonlinear Sci. 1 (1991) 17-70.

[35] H. Petryk, S. Stupkiewicz, Interfacial energy and dissipation in martensitic phase transformations. Part I: Theory Journal of the Mechanics and Physics of Solids 58 (2010) 390– 408.

[36] H. Gu, L. Bumke, C. Chluba, E. Quandt, R. D. James, Phase engineering and supercompatibility of shape memory alloys, Materials Today 21 (2018) 265-277.

[37] J. C. Lashley, S. M. Shapiro, B. L. Winn, C. P. Opeil, M. E. Manley, A. Alatas, W. Ratcliff, T. Park, R. A. Fisher, B. Mihaila, P. Riseborough, E. K. H. Salje, J. L. Smith, Observation of a Continuous Phase Transition in a Shape-Memory Alloy, Physical Review Letters 101 (2008) 135703.

[38] A. Zheludev, S. M. Shapiro, P. Wochner, A. Schwartz, M. Wall, L. E. Tanner, Phonon anomaly, central peak, and microstructures in Ni_2MnGa, Phys. Rev. B 51, 11310 (1995).

[39] L. Isaeva, P. Souvatzis, O. Eriksson, J. C. Lashley, Lattice dynamics of cubic AuZn from first principles, Phys. Rev. B 89 (2014) 104101.

Graphic Abstract